PCCP

Accepted Manuscript

ROYAL SOCIETY OF CHEMISTRY

www.rsc.org/pccp

Effects of GPI-anchored TNAP on the dynamic structure of model membranes

Garcia A.F.[a,#], Simão, A.M.S[b,#], Bolean, M.[b], Hoylaerts, M. F.[c], Millán, J.L.[d], Ciancaglini, P.[b] and Costa-Filho, A.J.[a,*]

[a] Laboratório de Biofísica Molecular, Departamento de Física, Faculdade de Filosofia, Ciências e Letras de Ribeirão Preto, Universidade de São Paulo, Ribeirão Preto, SP, Brasil

[b] Departamento de Química , Faculdade de Filosofia, Ciências e Letras de Ribeirão Preto, Universidade de São Paulo, Ribeirão Preto, SP, Brazil

[c] Center for Molecular and Vascular Biology, University of Leuven, Leuven, Belgium

[d] Sanford Children's Health Research Center, Sanford - Burnham Medical Research Institute, La Jolla, CA, USA

[#]These authors contributed equally to this work

*Corresponding author: Antonio José Costa-Filho,
Dep. Física, FFCLRP-USP;
Av. Bandeirantes, 3900,
14040-901; Ribeirão Preto, SP, Brasil
FAX: +55 16 36024838
E-mail: ajcosta@ffclrp.usp.br

Abstract

Tissue-nonspecific alkaline phosphatase (TNAP) plays a crucial role during skeletal mineralization, and TNAP deficiency leads to the soft bone disease hypophosphatasia. TNAP is anchored to the external surface of the plasma membranes by means of a GPI (glycosylphosphatidylinositol) anchor. Membrane-anchored and solubilized TNAP displays different kinetic properties against physiological substrates indicating that membrane-anchoring influences enzyme function. Here, we used Electron Spin Resonance (ESR) along with spin labeled phospholipids to probe possible dynamic changes prompted by the interaction of GPI-anchored TNAP with model membranes. The goal was to systematically analyze the ESR data in terms of line shape changes and of alterations in parameters such as rotational diffusion rates and order parameters obtained from non-linear least-square simulations of the ESR spectra of probes incorporated into DPPC liposomes and proteoliposomes. Overall, the presence of TNAP increased the dynamics and decreased ordering in the three distinct regions probed by the spin labeled lipids DOPTC (headgroup), 5-, and 16-PCSL (acyl chains). The largest change was observed for 16-PCSL, thus suggesting that GPI-anchored TNAP can give rise to long reaching modifications that could influence membrane processes halfway through the bilayer.

Introduction

Alkaline phosphatases belong to a multigene family encoded in humans by 4 distinct gene loci: *ALPP*, *ALPP2* and *ALPI* genes encode the placental, germ cell and intestinal isozymes, while *ALPL* encodes the tissue-nonspecific alkaline phosphatase isozyme, also known as liver-bone-kidney type [1]. *In vivo*, TNAP plays a crucial role during the process of endochondral ossification restricting the concentration of inorganic pyrophosphate (PP_i), a potent mineralization inhibitor [2-4]. Hypomorphic mutations in *ALPL* lead to hypophosphatasia, an inherited error of metabolism characterized by soft bones in children and/or adults (rickets or osteomalacia) due to accumulation of PP_i in the extracellular matrix [5]. *In vitro*, TNAP is a nonspecific phosphomonohydrolase (E.C.3.1.3.1) able to hydrolyze phosphate monoesters (ATP, ADP, AMP, p-nitrophenylphosphate, glucose-6-phosphate, glucose-1-phosphate, glyceraldehyde-3-phosphate), PP_i, phosphate diesters (bis-p-nitrophenylphosphate and cyclic AMP) and to catalyze transphosphorylation reactions [6-19].

Regardless of their tissue of origin, alkaline phosphatases are homodimeric enzymes and each catalytic site has three metal ions (two zinc ions and one magnesium ion) required for the enzymatic activity [1, 20-22]. Studies regarding the involvement of TNAP in the calcification process have suggested that the enzyme can be found either in a soluble form or associated to membranes [18, 23-26]. TNAP is associated with the membrane through a glycosylphosphatidylinositol (GPI) anchor. The anchor structure provides lateral mobility in the membrane and allows for TNAP release by the action of phospholipases [1, 13, 18].

Our research group has demonstrated that the catalytic properties of TNAP vary depending on the microenvironment where the enzyme is located. Thus, different forms of the enzyme (membrane-bound, detergent-solubilized or phospholipase-treated) show different specificities for the various substrates, suggesting that the enzyme's kinetic

properties are significantly affected by the presence of the GPI anchor and/or other membrane components [27-32]. However, little is known about the effects of the GPI anchor on the dynamic properties of the membrane's acyl chains. To address this issue we carried out an ESR study using spin labeled phospholipids that allow monitoring the headgroup region (DOPTC) and two different positions along the lipid acyl chain (n-PCSL). Spectral simulations of the ESR spectra measured before and after TNAP addition to a membrane mimetic were used to assess the profiles of ordering and molecular mobility of the membrane in the presence of the GPI-anchored protein.

Materials and Methods

Materials

Mammalian CHO-K1 cells were purchased from Rio de Janeiro Cell Bank (Rio de Janeiro, RJ). Spin labels DOPTC (1,2-dipalmitoyl-sn-glycero-3-phosphocholine) and n-PCSL (1-acyl-2-[n-(4,4-dimethyloxazolidine-N-oxyl)stearoyl]-sn-glycero-3-phosphocholine) with n=5 and 16, were purchased from Avanti Polar Lipids. Synthetic phosphatidylcholine DPPC (1,2-dipalmitoyl-sn-glycero-3-phosphocholine) was from Avanti Polar Lipids (Alabaster, AL). The chemical structures of the labeled lipids can be found elsewhere[33]. Organic solvents and other chemicals were from Sigma-Aldrich.

Cell culture and preparation of membrane fractions rich in TNAP

Cells were prepared and cultured according to Simão et al [28]. Membrane-bound recombinant human TNAP was obtained from transfected CHO-K1 cells as described by Simão et al [34].

Solubilization and partial purification of GPI-anchored TNAP with polyoxyethylene-9-lauryl ether (polidocanol)

Membrane-bound TNAP (0.2 mg/mL) was solubilized with 1% polidocanol (w/v, 10 mg/mL final concentration) for 1 h, with constant stirring, at 25ºC. After centrifugation at 100,000xg for 1 h at 4ºC, detergent-free solubilized enzyme was obtained using 200 mg of Calbiosorb resin and 1 mL of polidocanol-solubilized enzyme (~ 0.03 mg of protein/mL) as previously described [35]. All protein concentrations were estimated in the presence of 2% (w/v, 20 mg/mL) SDS [36]. Bovine serum albumin was used as a standard.

Liposome preparation and incorporation of GPI-anchored TNAP into liposomes

Dipalmitoyl phosphatidylcholine (DPPC) liposomes were prepared from a 10 mg/mL chloroform stock solution of lipids. Spin-labeled phosphatidylcholines were incorporated at a concentration of 0.5 mol % of total lipids by drying down the chloroform lipid solutions under a stream of nitrogen, followed by further drying in a SpeedVac Concentrator system (Thermo Scientific) overnight. The dried lipid film was resuspended in 50 mM Tris-HCl buffer, pH 7.5, containing 2 mM $MgCl_2$, and the mixture was incubated at 50ºC for 1 h, with vigorous stirring using a vortex at 10-min intervals. The mixture was passed through an extrusion system (Liposofast, Sigma) using a polycarbonate membrane of 100 nm, and the suspension of relatively homogeneous unilamellar vesicles was stored at 4ºC.

DPPC-proteoliposomes containing TNAP were prepared by mixing and incubating 1 mL of liposomes and 10 mL of detergent-free TNAP in 50 mM Tris-HCl buffer, pH 7.5, containing 2 mM $MgCl_2$ for 1 h, at 25ºC. The mixture was then centrifuged at 100,000xg for 1 h, at 4ºC. The pellet was resuspended in 0.5 mL of the

same buffer. TNAP activities in the supernatant and in the resuspended pellet were assayed and used to calculate the percentage of protein incorporation. *p*-nitrophenylphosphate (*p*NPP) activity for TNAP was assayed discontinuously, at 37ºC, in a spectrophotometer by following the release of *p*-nitrophenolate ion as described before [19, 34, 37].

Enzymatic release of TNAP from proteoliposome was performed as described before by Pizauro et al. [13, 27, 29, 34, 35]. The proteoliposomes were incubated in 50 mmol/L Tris–HCl buffer, pH 7.5 with specific phosphatidylinositol phospholipase C (0.1 U of PIPLC from *B. thuringiensis*) for 1 h under constant rotary shaking, at 37 °C. The incubation mixture was centrifuged at 100,000×g for 1 h, at 4 °C.

Electron spin resonance (ESR) measurements

Continuous wave ESR spectroscopy was carried out at room temperature (22 ± 1 °C) on a Jeol JES-FA200 spectrometer operating at X-band (9.2 GHz). Solutions containing TNAP incorporated in the spin-labeled DPPC liposomes were drawn into capillary tubes for ESR experiments. All ESR spectra were measured with the following experimental parameters: field range of 100 G, microwave frequency of 9.2 GHz, modulation frequency of 100 kHz, modulation amplitude of 100 kHz, and microwave power of 10 mW. The ESR spectra were processed utilizing OriginPro8 software.

Spectral simulations of the ESR spectra were performed using the NLSL program developed by Freed et al [38] and available for download at http://www.acert.cornell.edu/index_files/acert_resources.php. The simulations yielded the average rotational diffusion rate R_1 and the coefficients c_{20} and/or c_{22} of an orienting potential experienced by the nitroxide moiety. Order parameters, S_0 and/or S_2, can be calculated from those coefficients as described elsewhere [38]. Other parameters used as

input in the simulations, such as magnetic tensor (g- and hyperfine) components, were obtained from previously published data [38]. The fitting procedure followed similar strategies as those described in Basso et al [39]. To avoid local minima and to obtain error estimates for each varied parameter, the fits were initiated from different sets of seed values. Once minimization of the parameters was concluded, their final values were compared and their average along with the respective standard deviation were used as final results [40]. The procedure led to percent error estimates of: R1 (2 %) and order parameter (5 %).

Results

Several reports suggest that lipid membrane composition can modulate TNAP phosphomonohydrolase activity [27-30, 32]. In addition, evidences indicate TNAP is found in special regions of the membrane called lipid rafts, microdomains rich in cholesterol and sphingomyelin [1, 41-43, 44, 45]. However, the docking mechanisms of most GPI-anchored proteins, such as TNAP, and the possible effects of this anchoring mechanism on the enzymatic activity are still unclear.

Sharom et al. [46] used Förster resonance energy transfer (FRET) to examine the anchoring of PLAP and concluded that the GPI-anchored protein is close to the membrane bilayer and the calculated distance was about 10 Å from the membrane. Here, we used ESR of labeled phospholipids to examine the anchoring mechanism of TNAP. The line shape of the ESR spectrum is very sensitive to the spin label ordering and dynamics in membrane bilayers [47-51]. Moreover, spectral simulations, based on the routines developed by Freed et al [38], allow for a detailed quantification of both ordering and dynamics.

The headgroup region of the membrane models was probed by DOPTC spin label and the corresponding ESR spectra of DOPTC incorporated in liposomes of pure DPPC or in proteoliposomes harboring TNAP are shown in Figure 1. A qualitative analysis of these DOPTC ESR spectra indicates that the three typical lines observed in the nitroxide spectrum become narrower in the presence of TNAP, suggesting the spin probes are undergoing a somewhat faster motion. To clearly quantify this finding we performed NLSL simulations of both spectra. The best fits to the experimental data are seen as red lines in Figure 1. From the fits, an R_1 value of 0.11×10^9 s^{-1}, which corresponds to a correlation time of 3.30 ns, and an order parameter of ca. 0.37 were found. In the presence of TNAP, R_1 is increased to 0.16×10^9 s^{-1} (τ_c 2,23 ns) and ordering is reduced to 0.30. Hence, when TNAP is in the membrane mimetic, ordering and dynamics are changed such that the spin probes are in a more fluid and less ordered environment at the headgroup region. This result suggests that the enzyme itself does not touch the membrane surface thus allowing for the headgroup to experience a less hindered motion that leads to slightly higher dynamics and less ordering.

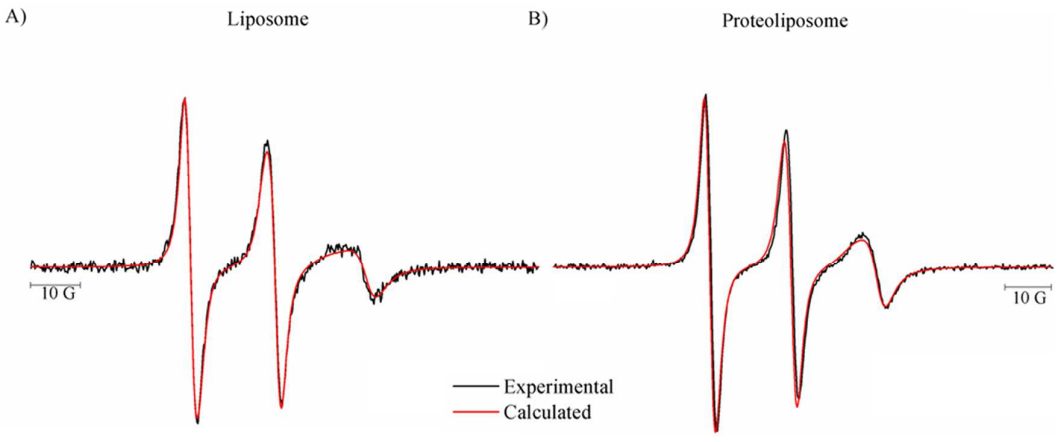

Figure 1 – Room temperature ESR spectra (black line) along with the best fit (red line) from the NLSL simulations of DOPTC spin probe incorporated in DPPC-liposome (A) and of DOPTC incorporated in DPPC-proteoliposome containing TNAP. Lipid/protein ratio was 1/8,000.

Besides probing the headgroup of the phospholipids with DOPTC, we also checked for changes in the lipid carbon acyl chains of the membrane caused by the presence of GPI-anchored TNAP. To do so we used two additional spin probes: one with nitroxide radical at carbon 5 (close to the water/lipid interface) and the other with the probe at carbon 16 (at the end of the acyl chain).

The environment probed by 5-PCSL is closer to the membrane surface, where the nitroxide radicals are subjected to a natural more restricted motion due to the higher degree of packing of the bilayer [52]. This more restricted type of motion is clearly reflected in the low-field line of the 5-PCSL ESR spectrum (Figure 2) in the absence of the enzyme. The lines are much broader and the lineshape much "distorted" than those observed for DOPTC. The simulation of 5-PCSL spectrum in the control experiment yielded an R_1 value of 0.083×10^9 s^{-1} (τ_c of 2.00 ns), in agreement with our qualitative observation of slower dynamics probed by 5-PCSL when compared to DOPTC, and an order parameter of 0.32. A lineshape change is observed in the presence of GPI-anchored TNAP. The simulation also shows such alteration with the R_1 value increasing slightly to 0.091×10^9 s^{-1} (τ_c of 1.83 ns) and the order parameter decreasing to 0.24.

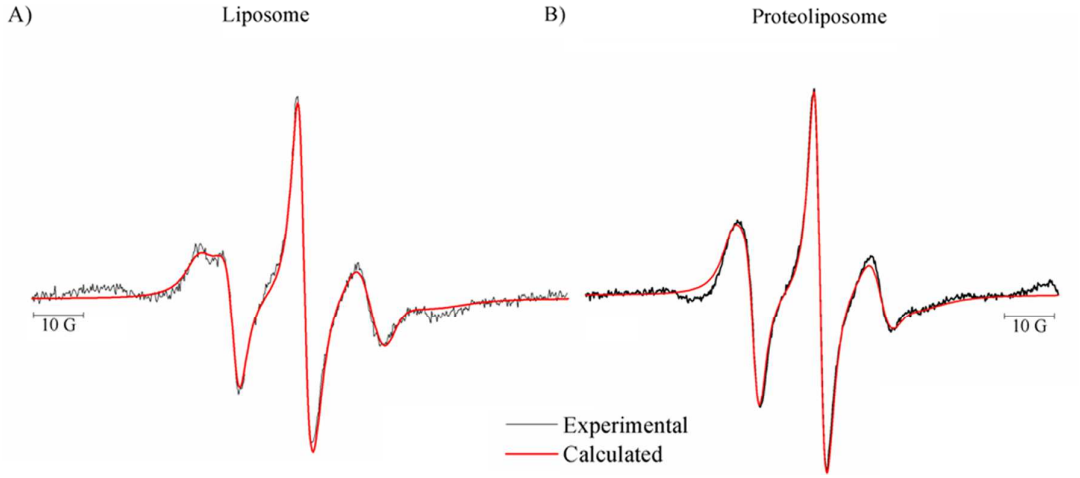

Figure 2 – Room temperature ESR spectra (black line) along with the best fit (red line) from the NLSL simulations of 5-PCSL incorporated in DPPC-liposome (A) and of 5-PCSL incorporated in DPPC-proteoliposome containing TNAP. Lipid/protein ratio was 1/8,000.

Finally, the spin-labeled phospholipid 16-PCSL was used to probe TNAP-induced alterations further down the acyl chain. 16-PCSL is located in the middle of the bilayer and thus gives rise to ESR spectra associated with much higher mobility than the other probes used in this work. This is clearly seen in its spectra (Figure 3) that present sharp and intense lines, especially the low- and mid-field resonances, whose intensity ratio is closer to one (this ratio can be used as a measure of label mobility). To quantify the order and dynamics of the labels in the absence and in the presence of TNAP, NLSL simulations of the spectra in Figure 3 were again performed. The best fit to the experimental spectrum in the absence of the enzyme was achieved with an R_1 value of 0.66×10^9 s^{-1} and a negligible order parameter of 0.06. It can be readily seen that this is the fastest regime of motion observed amongst the different regions probed by the set of labels chosen in this paper. In the presence of the GPI-anchored TNAP, the ESR spectrum shows differences in its line shape that qualitatively indicate an increase in dynamics (low- and mid-field line intensities become very similar). The simulation of the spectrum led to R_1 of 2.40×10^9 s^{-1} and again a negligible order parameter of 0.04.

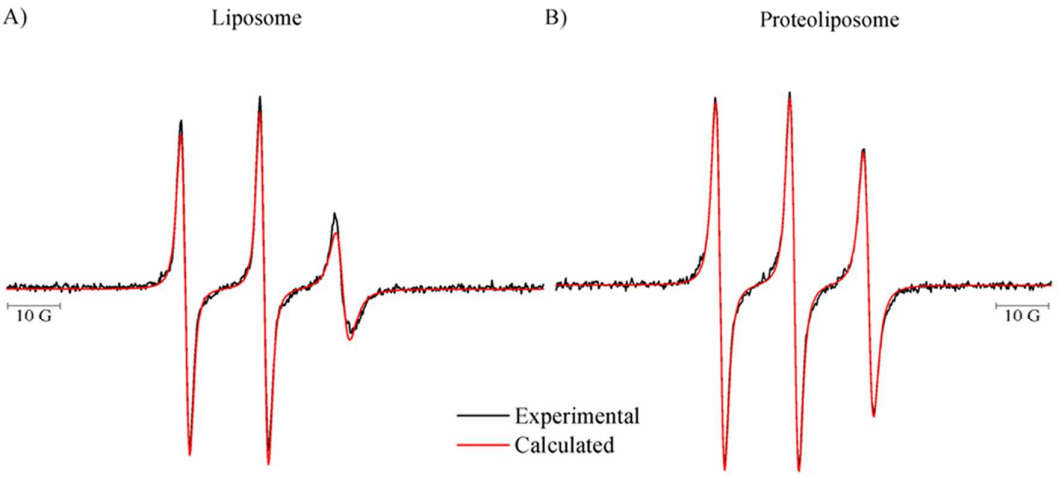

Figure 3 – Room temperature ESR spectra (black line) along with the best fit (red line) from the NLSL simulations of 16-PCSL incorporated in DPPC-liposome (A) and 16-PCSL incorporated in DPPC-proteoliposome containing TNAP. Lipid/protein ratio was 1/8,000.

Discussions

The use of spin labeled lipids and ESR has proved to be one of the most valuable spectroscopic methods for studying protein interactions with biological membranes. This is due to the sensitivity of spin label ESR to dynamics in the ns timescale [53]. In this sense the studies of GPI-anchored TNAP performed here using ESR allowed us to get valuable insights on the effects caused by the presence of TNAP on the dynamic organization of lipids in the membrane mimetic system. Previous studies, such as those reported by Ciancaglini's [27, 29, 32] and by Roux's group[44, 45, 54], have dealt with the same problem. However, here we can dissect the effects of TNAP presence as a function of the depth within the bilayer due to the localization of the spin label moiety in very specific region of the bilayer, especially for DPPC membranes in the gel phase. Furhermore, Murphy and Messersmith[55] have shown that DPPC liposomes are an adequate initial choice of model of matrix vesicles involved in biomineralization.

The ESR spectra for all probes used in DPPC-containing models revealed that the enzyme increased the membrane dynamics and decreased the bilayer order (Figure 4). The quantitative results obtained from the NLSL simulations of the ESR spectra are expressed in terms of the rotational diffusion rate (R_1), interpreted as the fluidity of the membrane, and the order parameter. From these values, we can see that the presence of the GPI-anchored TNAP led to intermediate increases of R_1 at the polar head group (from 0.11×10^9 s^{-1} to 0.16×10^9 s^{-1}) and in the region closer to the bilayer surface (from 0.083×10^9 s^{-1} to 0.091×10^9 s^{-1}), whereas the order parameters reported a decrease in both cases. This means that the lipids experience a higher degree of freedom to move around when TNAP is present, which induces a smaller orienting potential and higher fluidity [29] (Figure 4). In particular at the head group, the increase in R_1 and the decrease of the order parameter indicate that the TNAP structure itself does not lie on the surface of the membrane as also observed for PLAP by Sharom et al. ~~using FRET techniques~~ [46] and for another GPI-anchored alkaline phosphatase by Ronzon et al.[54]

The largest change observed in our ESR results comes from the dramatic increase of the R_1 values for the 16-PCSL probes. These probes are located half way through the bilayer and are naturally in a more fluid and less ordered environment when compared to the probes that report on other regions of the bilayer as one can see from the R_1 values obtained from pure DPPC liposomes. In our case, 16-PCSL is not submitted to an orienting potential, which gives rise to close to zero values of the order parameter that were not affected much by the presence of the GPI-anchored enzyme (it changes from 0.06 to 0.04). However, R_1 values showed a four-fold increase when TNAP is in the proteoliposomes, changing from 0.66×10^9 s^{-1} to 2.40×10^9 s^{-1}. This result indicates that the GPI-anchored TNAP is able to affect the bilayer organization deep down to the end of the lipid acyl chain, inducing higher fluidity (Figure 4).

Ronzon et al[56] showed that GPI-anchored alkaline phosphatase was able to disorder the hydrocarbon chains of DPPS monolayers in a much more pronounced way than for DPPC monolayers. Here, using ordered DPPC bilayers, we showed TNAP is capable of perturbing the whole extension of the acyl chains with a great effect right in the middle of the bilayer. Any process that needs some sort of long extent change within the bilayer can then be affected by the presence of TNAP and its GPI-anchor. For example, GPI-anchored TNAP has the ability to spontaneously insert into the lipid bilayer and several reports have suggested that this protein associates preferentially with cholesterol- and sphingolipid-rich regions called raft domains [29, 32, 37, 57]. It has been proposed that acyl and alkyl chain lengths of GPI-anchors in proteins could determine raft association [58]. Thus, the length and order of aliphatic chains in both the fluid and the ordered phases are expected to affect the GPI-anchored protein-domain interactions and the fluidity changes induced by TNAP could be related to the recruitment and to the association of other raft related proteins like Annexins. Moreover, since TNAP has been shown to preferentially partition in lipid ordered domains, our results could be extended to reveal the effect of TNAP presence on the dynamic structure of ordered bilayers such as DPPC in the gel phase liposomes used in this study.

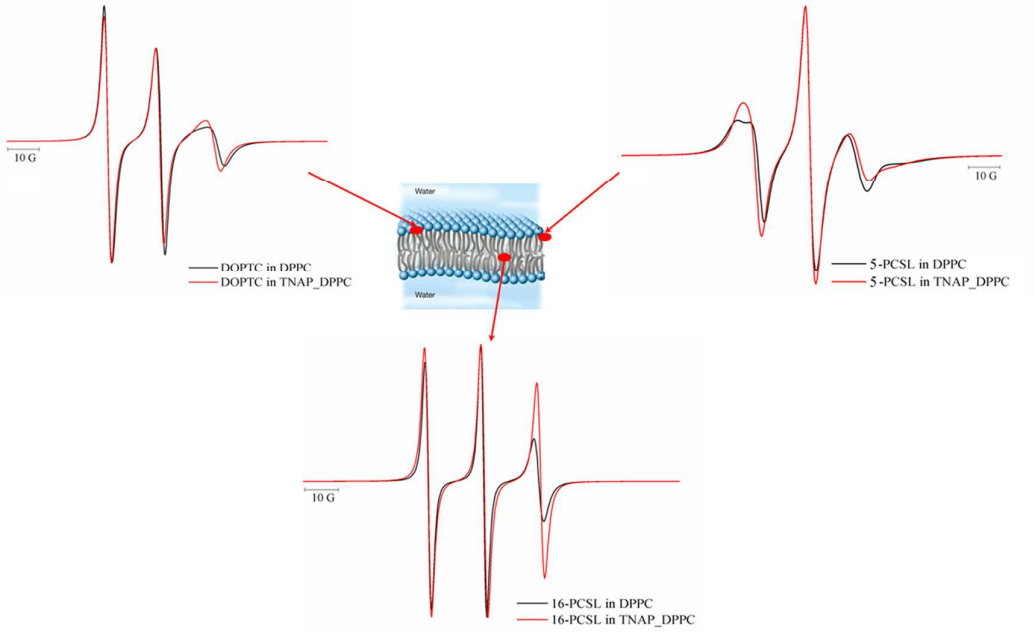

Figure 4 – Comparison of ESR best fits from NLSL simulations of DOPTC, 5-PCSL and 16-PCSL incorporated in DPPC-liposome (black line) and DPPC-proteoliposome containing TNAP (red line) emphasizing the spectral changes induced by TNAP.

In order to check whether the observed changes were due to the presence of the whole GPI-anchored TNAP structure or whether they could also be induced by the GPI motif only, the TNAP-containing proteoliposomes were treated with PIPLC from *B. thuringiensis*, which cleaves specifically GPI anchors, allowing a selective release of the TNAP protein chain to the solution [13, 29, 59]. This sample was then submitted to ESR experiments using DOPTC and 5-PCSL probes. The corresponding spectra are shown in Figure 5 and one can see there were much smaller changes in this case. About 70% of TNAP activity was lost after the treatment (data not showed), indicating TNAP is not completely removed from the proteoliposomes and the smaller changes observed in Figure 5 could be attributed to the presence of GPI-anchored TNAP that remained in the sample even after treatment. This result highlights the importance of having the whole protein structure along with the GPI motif in order to promote in full the alterations described above.

Our data underscore the importance of obtaining direct structural information on this physiologically relevant GPI-anchored enzyme in a lipid bilayer environment. We conclude that TNAP is probably close to the membrane surface and that this proximity can be related to the modulation of catalytic activity by the lipid composition as previously reported [27-30, 32, 52]. Further studies are necessary to fully understand the implications of the GPI-anchoring mechanism on TNAP structure and function and on membrane protein organization in matrix vesicles.

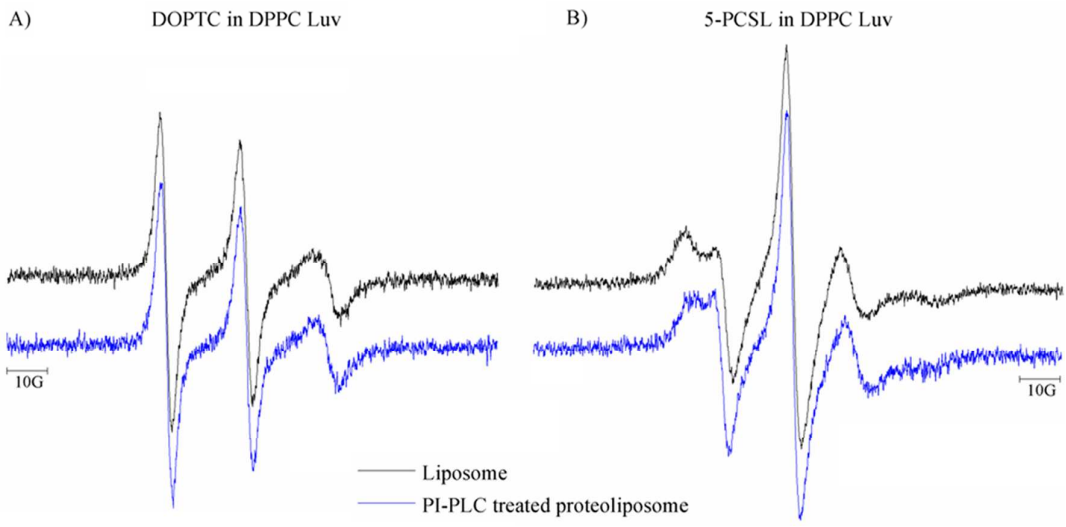

Figure 5 – Room temperature ESR spectra from (A) DOPTC and (B) 5-PCSL incorporated in DPPC liposomes. Pure liposomes treated with PIPLC protease (black line) and TNAP proteoliposomes treated with PIPLC protease (blue line).

Acknowledgements

This work was supported in part by grants DE12889 and AR53102 from the National Institutes of Health, USA. We also thank FAPESP (2010/17662-8, 2013/26088-1, 2014/00371-1 and 2014/11941-3), CAPES and CNPq for the financial support given to our laboratory. AMSS received a CAPES scholarship. GAF and MB received FAPESP scholarship. PC and AJCF also acknowledge CNPq for research

fellowships.

References

1. J. L. Millan, *Purinergic signalling*, 2006, **2**, 335-341.
2. M. Murshed, D. Harmey, J. L. Millan, M. D. McKee and G. Karsenty, *Genes Dev*, 2005, **19**, 1093-1104.
3. D. Harmey, L. Hessle, S. Narisawa, K. A. Johnson, R. Terkeltaub and J. L. Millan, *Am J Pathol*, 2004, **164**, 1199-1209.
4. L. Hessle, K. A. Johnson, H. C. Anderson, S. Narisawa, A. Sali, J. W. Goding, R. Terkeltaub and J. L. Millan, *Proc Natl Acad Sci U S A*, 2002, **99**, 9445-9449.
5. M. P. Whyte, C. R. Greenberg, N. J. Salman, M. B. Bober, W. H. McAlister, D. Wenkert, B. J. Van Sickle, J. H. Simmons, T. S. Edgar, M. L. Bauer, M. A. Hamdan, N. Bishop, R. E. Lutz, M. McGinn, S. Craig, J. N. Moore, J. W. Taylor, R. H. Cleveland, W. R. Cranley, R. Lim, T. D. Thacher, J. E. Mayhew, M. Downs, J. L. Millan, A. M. Skrinar, P. Crine and H. Landy, *N Engl J Med*, 2012, **366**, 904-913.
6. R. B. McComb, Bowers, G.N., Jr., Posen, S., *Plenum Press*, 1979.
7. H. H. Hsu, P. A. Munoz, J. Barr, I. Oppliger, D. C. Morris, H. K. Vaananen, N. Tarkenton and H. C. Anderson, *The Journal of biological chemistry*, 1985, **260**, 1826-1831.
8. C. Curti, J. M. Pizauro, P. Ciancaglini and F. A. Leone, *Cell Mol Biol*, 1987, **33**, 625-635.
9. J. M. Pizauro, C. Curti, P. Ciancaglini and F. A. Leone, *Comp Biochem Physiol B*, 1987, **87**, 921-926.
10. J. M. Pizauro, P. Ciancaglini and F. A. Leone, *Int J Biochem*, 1992, **24**, 1391-1396.
11. J. M. Pizauro, P. Ciancaglini and F. A. Leone, *Biochimica et biophysica acta*, 1993, **1202**, 22-28.
12. J. M. Pizauro, P. Ciancaglini and F. A. Leone, *Braz J Med Biol Res*, 1994, **27**, 453-456.
13. J. M. Pizauro, P. Ciancaglini and F. A. Leone, *Mol Cell Biochem*, 1995, **152**, 121-129.
14. P. Ciancaglini, J. M. Pizauro, C. Curti, A. C. Tedesco and F. A. Leone, *Int J Biochem*, 1990, **22**, 747-751.
15. A. A. Rezende, J. M. Pizauro, P. Ciancaglini and F. A. Leone, *Biochem J*, 1994, **301 (Pt 2)**, 517-522.
16. F. A. Leone, L. A. Rezende, P. Ciancaglini and J. M. Pizauro, *Int J Biochem Cell Biol*, 1998, **30**, 89-97.
17. L. A. Rezende, P. Ciancaglini, J. M. Pizauro and F. A. Leone, *Cell Mol Biol (Noisy-le-grand)*, 1998, **44**, 293-302.
18. F. A. Leone, P. Ciancaglini and J. M. Pizauro, *J Inorg Biochem*, 1997, **68**, 123-127.
19. P. Ciancaglini, J. M. Pizauro and F. A. Leone, *J Inorg Biochem*, 1997, **66**, 51-55.
20. B. Stec, A. Cheltsov and J. L. Millan, *Acta Crystallogr Sect F Struct Biol Cryst Commun*, 2010, **66**, 866-870.
21. M. H. Le Du and J. L. Millan, *The Journal of biological chemistry*, 2002, **277**, 49808-49814.
22. M. H. Le Du, T. Stigbrand, M. J. Taussig, A. Menez and E. A. Stura, *The Journal of biological chemistry*, 2001, **276**, 9158-9165.
23. G. W. Cyboron and R. E. Wuthier, *The Journal of biological chemistry*, 1981, **256**, 7262-7268.
24. R. E. Wuthier, J. E. Chin, J. E. Hale, T. C. Register, L. V. Hale and Y. Ishikawa, *The Journal of biological chemistry*, 1985, **260**, 15972-15979.
25. C. Curti, J. M. Pizauro, G. Rossinholi, I. Vugman, J. A. Mello de Oliveira and F. A. Leone, *Cell Mol Biol*, 1986, **32**, 55-62.
26. J. C. Say, K. Ciuffi, R. P. Furriel, P. Ciancaglini and F. A. Leone, *Biochimica et biophysica acta*, 1991, **1074**, 256-262.
27. M. Bolean, A. M. Simao, B. Z. Favarin, J. L. Millan and P. Ciancaglini, *Biophysical chemistry*, 2011, **158**, 111-118.
28. A. M. Simao, M. C. Yadav, S. Narisawa, M. Bolean, J. M. Pizauro, M. F. Hoylaerts, P. Ciancaglini and J. L. Millan, *The Journal of biological chemistry*, 2010, **285**, 7598-7609.
29. M. Bolean, A. M. Simao, B. Z. Favarin, J. L. Millan and P. Ciancaglini, *Biophysical chemistry*, 2010, **152**, 74-79.
30. P. Ciancaglini, A. M. Simao, F. L. Camolezi, J. L. Millan and J. M. Pizauro, *Braz J Med Biol Res*, 2006, **39**, 603-610.

31. T. Kiffer-Moreira, C. R. Sheen, K. C. Gasque, M. Bolean, P. Ciancaglini, A. van Elsas, M. F. Hoylaerts and J. L. Millan, *PLoS One*, 2014, **9**, e89374.
32. P. S. Ciancaglini, A. M. S. ; Bolean, M. ; Millán, J. L. ; Rigos, C. F. ; Yoneda, J. S. ; COLHONE, M. C. ; Stabeli, R. G. , *Biophysical Reviews*, 2012, **v. 4**, p. 67-81.
33. S. G. Couto, M. C. Nonato and A. J. Costa-Filho, *Biophysical Journal*, 2008, **94**, 1746-1753.
34. A. M. Simao, M. M. Beloti, A. L. Rosa, P. T. de Oliveira, J. M. Granjeiro, J. M. Pizauro and P. Ciancaglini, *Cell Biol Int*, 2007, **31**, 1405-1413.
35. F. L. Camolezi, K. R. P. Daghastanli, P. P. Magalhaes, J. M. Pizauro and P. Ciancaglini, *Int J Biochem Cell B*, 2002, **34**, 1091-1101.
36. E. F. Hartree, *Anal Biochem*, 1972, **48**, 422-427.
37. P. Ciancaglini, M. C. Yadav, A. M. Simao, S. Narisawa, J. M. Pizauro, C. Farquharson, M. F. Hoylaerts and J. L. Millan, *J Bone Miner Res*, 2010, **25**, 716-723.
38. D. J. Schneider, and J. H. Freed. L. J. , *In Biological Magnetic Resonance.*, 1989, **8**, 1-76.
39. L. G. M. Basso, R. Z. Rodrigues, R. Naal and A. J. Costa, *Biochimica Et Biophysica Acta-Biomembranes*, 2011, **1808**, 55-64.
40. A. J. Costa, R. H. Crepeau, P. P. Borbat, M. T. Ge and J. H. Freed, *Biophysical Journal*, 2003, **84**, 3364-3378.
41. T. Endo, *Tanpakushitsu Kakusan Koso*, 1992, **37**, 1988-1992.
42. R. M. Henderson, J. M. Edwardson, N. A. Geisse and D. E. Saslowsky, *News Physiol Sci*, 2004, **19**, 39-43.
43. M. C. Giocondi, F. Besson, P. Dosset, P. E. Milhiet and C. Le Grimellec, *J Mol Recognit*, 2007, **20**, 531-537.
44. S. Morandat, M. Bortolato and B. Roux, *Biochimica Et Biophysica Acta-Biomembranes*, 2002, **1564**, 473-478.
45. P. E. Milhiet, M. C. Giocondi, O. Baghdadi, F. Ronzon, B. Roux and C. Le Grimellec, *Embo Reports*, 2002, **3**, 485-490.
46. F. J. Sharom and M. T. Lehto, *Biochem Cell Biol*, 2002, **80**, 535-549.
47. F. Dyszy, A. P. Pinto, A. P. Araujo and A. J. Costa-Filho, *PLoS One*, 2013, **8**, e60198.
48. L. Mainali, J. B. Feix, J. S. Hyde and W. K. Subczynski, *J Magn Reson*, 2011, **212**, 418-425.
49. S. G. Couto, M. Cristina Nonato and A. J. Costa-Filho, *Biochem Biophys Res Commun*, 2011, **414**, 487-492.
50. D. Marsh, *Mol Biol Biochem Biophys*, 1981, **31**, 51-142.
51. M. Ge, A. Gidwani, H. A. Brown, D. Holowka, B. Baird and J. H. Freed, *Biophys J*, 2003, **85**, 1278-1288.
52. P. Jurkiewicz, A. Olzynska, L. Cwiklik, E. Conte, P. Jungwirth, F. M. Megli and M. Hof, *Biochimica et biophysica acta*, 2012, **1818**, 2388-2402.
53. M. Esmann, A. Watts and D. Marsh, *Biochemistry*, 1985, **24**, 1386-1393.
54. F. Ronzon, S. Morandat, B. Roux and M. Bortolato, *Journal of Membrane Biology*, 2004, **197**, 169-177.
55. W. L. Murphy and P. B. Messersmith, *Polyhedron*, 2000, **19**, 357-363.
56. F. Ronzon, B. Desbat, J. P. Chauvet and B. Roux, *Biochimica Et Biophysica Acta-Biomembranes*, 2002, **1560**, 1-13.
57. M. C. Giocondi, B. Seantier, P. Dosset, P. E. Milhiet and C. Le Grimellec, *Pflug Arch Eur J Phy*, 2008, **456**, 179-188.
58. M. C. Giocondi, D. Yamamoto, E. Lesniewska, P. E. Milhiet, T. Ando and C. Le Grimellec, *Biochimica et biophysica acta*, 2010, **1798**, 703-718.
59. Y. W. Wong and M. G. Low, *Biochem J*, 1994, **301 (Pt 1)**, 205-209.